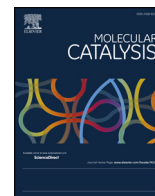




Contents lists available at ScienceDirect

Molecular Catalysis

journal homepage: www.elsevier.com/locate/mcat

Isoamyl acetate preparation from reaction of vinyl acetate and Isoamyl alcohol catalyzed by H-ZSM-5 zeolite: a kinetic study

Pablo F. Corregidor*, Delicia E. Acosta, Elio E. Gonzo, Hugo A. Destéfani

Facultad de Ingeniería, Instituto de Investigaciones para la Industria Química – INIQUI (UNSa-CONICET), Centro Científico Tecnológico (CCT) Salta, Consejo de Investigaciones de la UNSa (CIUNSa), Universidad Nacional de Salta, Av. Bolivia 5150, A4408FVYA Salta, Argentina

ARTICLE INFO

Keywords:

Transesterification
Isoamyl acetate
ZSM-5
Kinetic study

ABSTRACT

Microporous H-ZSM-5 zeolite having good crystallinity and with the presence of Brønsted acid sites exclusively, was prepared by hydrothermal treatment of Expanded Perlite. The as-prepared H-ZSM-5 was used as heterogeneous catalyst for the reaction between vinyl acetate and isoamyl alcohol, as a greener alternative for the traditional preparation of isoamyl acetate. In this reaction, isoamyl acetate was generated by an acyl nucleophilic substitution mechanism, mediated by an acetylated zeolite complex, while acetaldehyde diisoamyl acetal has been produced as a secondary product due to a nucleophilic addition to acetaldehyde carbonyl carbon. The reaction was studied under different alcohol/ester molar ratio, supporting a second order kinetics when working under excess of one reactant. Moreover, an Eley-Rideal kinetic model has been suggested for a reaction mechanism of five steps, involving the ketalization of isoamyl alcohol and acetaldehyde as a parallel reaction that competes with transesterification.

Introduction

A Fischer's esterification is a special type of reaction where a nucleophilic acyl substitution takes place over a carboxylic acid (RCOOH) based on the electrophilicity of the carbonyl carbon, which usually activates over an acidic catalyst. A possible mechanism for Fischer's esterification undergoes through the formation of a carbocation intermediate specie ($RC\equiv O^+$). This acylium ion is an electrophilic specie which further reacts with weak nucleophilic reagents such as alcohols to produce esters and water. This reaction was first described by Emil Fischer in 1895 as a thermodynamically reversible process in which products and reactants remain in an equilibrium state [1].

The extensive application in industry is the crucial feature of esterification that particularly differentiates from other reactions [2]. Nevertheless, some carboxylic acids have a low solubility in organic solvents which is difficult to carry out a homogeneous esterification, whereas esters are normally soluble in most of organic solvents. In that sense, a transesterification reaction is more advantageous than the ester synthesis from carboxylic acids and alcohols [3]. Thus, a transesterification is a classic organic reaction that has revealed a lot of industrial applications and laboratory purposes. The ester-to-ester transformation involved a reaction between an ester (R'COOR'') and an alcohol (ROH), this is particularly advantageous when the pair carboxylic acids are easily altered and difficult to isolate. Some esters, especially methyl and

ethyl esters are commercially accessible and thus they can be conveniently employed as starting materials in transesterification.

A transesterification reaction can also be studied as an acyl transfer-process where an ester relocates its acyl moiety over a reactant alcohol (acyl acceptor). This reaction remains at equilibrium in organic media and can be shifted in the desired direction in order to improve the conversion of reaction. In some cases, the use of a large excess of the acyl donor or the removal of one of the products are options to drive the process to completion. However, in practice, a more common solution is the use of activated esters, which ensure a more or less irreversible reaction. One of the best activated acyl donors are enol esters such as vinyl acetate [4,5]. In this case, the resultant product is vinyl alcohol, which simply tautomerizes to acetaldehyde [6]. The last one is a low-boiling point aldehyde that easily evaporates above room temperature. Moreover, the generation of a keto-compound (a weak nucleophile) instead of an alcohol improves the non-reversibility of the process.

On the other hand, modern catalysis is moving to a clean chemistry due to high performance and environmental impact, thus, solid catalysts emerge as a competitive alternative to traditional chemical synthesis for the production of fine chemicals. In that sense, zeolites are well known as heterogeneous acid catalysts and also have proved good activity in transesterification reactions [7–10]. Unlike the acylium ion obtained in most of classical nucleophilic acyl substitutions involving homogeneous acid catalysts, there is evidence for the formation of an

* Corresponding author.

E-mail address: pcorregidor@unsa.edu.ar (P.F. Corregidor).

<https://doi.org/10.1016/j.mcat.2018.06.009>

Received 13 April 2018; Received in revised form 22 May 2018; Accepted 6 June 2018
2468-8231/ © 2018 Elsevier B.V. All rights reserved.

acylated surface over nanostructured heterogeneous catalyst such as heteropoly acids [11] and zeolites [12–15]. These authors agree that acylium cation is formed during acylation reactions over a zeolite catalyst, which can be stabilized by negative charged oxygen on the active site. This stabilized acylium ion could then react, i.e. in a bimolecular electrophilic aromatic substitution mechanism [14].

Therefore, based in previous reports where the acylated surface of a zeolite can perform acylation reactions, we studied the preparation of isoamyl acetate, one of the most important flavor compounds used in food industries because of its characteristic banana flavor, using a transesterification reaction as an alternative to the traditional Fischer's esterification mechanism. Thus, we evaluated the influence of initial concentration of reactants over a transesterification reaction, catalyzed by the acid form of a ZSM-5 zeolite, obtained by a greener method. Moreover, we studied some kinetics aspects related with a possible mechanism of reaction and proposed a kinetic model for the studied reaction, providing a molecular interpretation that complements and enriches the experimental results.

Experimental

Materials and reagents

Expanded perlite from San Antonio de los Cobres (Northwestern Argentina) was previously conditioned by washing with water, followed by grinding and sieving through a 230 mesh sieve before using as starting material. In order to obtain the appropriate $\text{SiO}_2/\text{Al}_2\text{O}_3$ molar ratio in the gel of synthesis, sodium silicate (Fisher; Na_2O 27.7 wt% with a $\text{SiO}_2/\text{Na}_2\text{O}$ ratio of 2:1, was used as additional Si source. A sodium form of a commercial ZSM-5 zeolite (ALSI-Penta SN-55, $\text{SiO}_2/\text{Al}_2\text{O}_3 = 23$) was used as a crystallization seed.

For the transesterification reaction, a solution of vinyl acetate (Sigma Aldrich, $\geq 99\%$) and isoamyl alcohol (Biopack, $\geq 98.5\%$) in toluene (Merck, GC), was employed. All reagents and materials were used as received.

Synthesis of the ZSM-5 catalyst

The Na-form of a ZSM-5 zeolite was synthesized as reported previously [16]. Basically, the expanded perlite was used as the only alumina source and sodium silicate as supplementary silica source. A small quantity (7% wt of the total amount of SiO_2) of seeding Na-ZSM-5 zeolite was added into the reaction mixture with vigorous mixing. The hydrothermal synthesis of ZSM-5 was performed at a reaction temperature of 453 K for 24 h in 20 mL Teflon-lined stainless steel-autoclaves. H_2SO_4 or NaOH aqueous solutions were used to adjust the pH to 10.2 and the $\text{Na}_2\text{O}/\text{SiO}_2$ desired molar ratio of the reaction mixture. The composition of the mother liquor was 40 SiO_2 :12 Al_2O_3 :0.38 Na_2O :45 H_2O .

Transforming Na-ZSM-5 zeolite into the H-form

The zeolite obtained in the Na-form was previously converted to the NH_4 -ZSM-5 form following the procedure described by Triantafyllidis et al. [17]. A 10 wt% solution of NH_4Cl at a ratio of 1:10 was used for the ion exchange process. This mixture was stirred at 353 K for 1 h, filtered and washed with Milli-Q water (182 M Ω cm). This exchange procedure was repeated three times. The solid was collected and dried at room temperature for 12 h. At the end, the NH_4 -form was converted into the H-ZSM-5 form by heating under air flow at 723 K overnight.

Characterization of the catalyst

The powder X-ray diffraction (XRD) patterns were recorded on a STOE STADI P instrument using $\text{CuK}\alpha$ radiation ($\lambda = 0.15415$ nm). Diffraction lines of 2θ between 5° and 45° were taken to confirm the

phase of ZSM-5 zeolite, and the degree of crystallinity was calculated by comparing the sum of the areas below the dominant peaks between 22° and 25° of 2θ in the as-prepared zeolite, with the sum of the areas above the reference ZSM-5 sample (ALSI-Penta SN-55, $\text{SiO}_2/\text{Al}_2\text{O}_3 = 23$).

The specific surface area and the porosity of the samples were determined from N_2 adsorption/desorption isotherms using the multi-point BET method. The samples were outgassed under vacuum at 623 K for 10 h prior to the measurements. The isotherms were obtained with a Quantachrome Quadrasorb SI automated gas adsorption system, at liquid nitrogen temperature. The external surface area and the micropore volume were determined from the adsorption branch of the isotherm using the t -plot method.

Crystal morphology and size were identified by Scanning Electron Microscopy (SEM) with a JEOL JSM-6480 LV microscope. Before measurement, all the samples were coated by gold sputtering.

The aluminum coordination state of the zeolite samples was confirmed by ^{27}Al magic angle spinning nuclear magnetic resonance (^{27}Al MAS NMR). The spectra were recorded on a Bruker Advance DSX400 spectrometer operating at a magnetic field strength of 9.4 T; 36,000 scans were accumulated with a spinning frequency of 20 kHz, a pulse length of 0.3 μs and a recycle delay of 100 ms. The ^{27}Al signals were referenced to an externally located 0.1 mol L $^{-1}$ aqueous solution of $[\text{Al}(\text{H}_2\text{O})_6]^{3+}$.

^{29}Si magic angle spinning nuclear magnetic resonance spectra (^{29}Si MAS NMR) were recorded by accumulating 4000 scans with a spinning frequency of 5 kHz, a pulse width of 5 μs and a pulse delay of 60 s on a Bruker AMX300 spectrometer working at 7.0 T. Tetramethylsilane was used as a chemical shift reference.

The strength and distribution of acid sites were tested by adsorption and programmed desorption of pyridine using infrared (IR) spectroscopy. The infrared spectra of the zeolite sample were recorded in a Nicolet 6700 spectrometer equipped with a DTGS detector (128 scans, 2 cm^{-1} resolution). A self-supporting wafer (of about 15 mg) of the sample was evacuated in a homemade vacuum infrared cell fitted with ZnSe windows. The wafer was dried at 673 K for 1 h under vacuum. During the cooling down of the sample, reference spectra were recorded at 623, 523, 423 and 323 K. The evacuated sample was saturated with about 25 mbar of pyridine vapor at 323 K. The saturated wafer was then evacuated at 323 K for 30 min. The temperature-programmed desorption of adsorbed amine was carried out at a heating rate of 5 $^\circ\text{C}\cdot\text{min}^{-1}$, maintaining the temperature at 423, 523 and 623 K for 30 min. Then, the infrared spectra of adsorbed pyridine were recorded at these temperatures. The corresponding reference spectra were subtracted from these spectra and the band intensities at 1540 and 1450 cm^{-1} wavenumbers were determined and assigned to bands of Brønsted and Lewis acid sites of adsorbed pyridine, respectively. The concentration of Brønsted and Lewis acid sites was calculated with the integral molar extinction coefficients of pyridine infrared absorption bands determined by Emeis [18].

Liquid phase reaction of vinyl acetate and isoamyl alcohol

The reaction of vinyl acetate with isoamyl alcohol was carried out in 10 mL tightly closed glass vials under vigorous stirring (1000 rpm) in a multiple-well parallel reaction block. In a typical run, a solution containing: vinyl acetate (0.10–1.00 mol L $^{-1}$), isoamyl alcohol (0.10–0.30 mol L $^{-1}$) and toluene (solvent) was injected to a sealed vial containing 110 mg of H-ZSM-5 at room temperature. Normally, a set of two experiments (experiment A and B) were performed to evaluate the influence of concentration in the studied reaction. In the first one (experiment A), the influence of the vinyl acetate concentration was varied from 0.10 mol L $^{-1}$ to 1.00 mol L $^{-1}$, while keeping constant the concentration of isoamyl alcohol at 0.10 mol L $^{-1}$. In a second experiment (experiment B), the influence of the isoamyl alcohol concentration (0.10–0.30 mol L $^{-1}$) was evaluated while the vinyl acetate was invariant (0.10 mol L $^{-1}$). These conditions were resumed in Table 3.

The reaction mixture was stirred and heated at 363 K for 3 h. Consequently, at defined times of reaction, an aliquot of 0.1 mL was taken from the system (every 5 min for the first 20 min, then at 30, 40 and 60 min and finally every 30 min from 60 to 180 min of reaction). These solutions were analyzed by gas chromatography (GC) on a Perkin Elmer gas chromatograph, model Claurus 580, equipped with a capillary column (Elite-5: 0.25 μm x 30 m x 0.25 mm i.d.) and a flame ion detector. The temperature profile of the GC analysis was: 5 min at 313 K, from 313 to 453 K at 20 degrees min^{-1} and finally keeping 1.0 min at 453 K. The identity of the reactants and products was confirmed by gas chromatography-mass spectrometry analysis (GC-MS) on Agilent 6890 N Gas Chromatograph (HP-5MS: 0.25 μm x 30 m x 0.25 mm i.d.) coupled to Agilent 5973 MSN Mass Spectrometer.

A blank test consisting in a reaction system of vinyl acetate and isoamyl alcohol in toluene with no catalyst, was carried out under the same temperature and stirring conditions as mentioned before. Less of 3% of conversion was obtained at nearly 24 h of reaction, undoubtedly proving that results obtained for catalyzed experiments are due to the activity of ZSM-5.

Conversions of isoamyl alcohol and vinyl acetate were calculated based on Eqs. (1) and (2), respectively:

$$\text{conversion of isoamyl alcohol (\%)} = \frac{\text{mol of isoamyl alcohol converted}}{\text{initial mol of isoamyl alcohol}} \cdot 100 \quad (1)$$

$$\text{conversion of vinyl acetate (\%)} = \frac{\text{mol of vinyl acetate converted}}{\text{initial mol of vinyl acetate}} \cdot 100 \quad (2)$$

Selectivity to isoamyl acetate was calculated according to Eq. (3).

$$S_{\text{isoamyl acetate}}(\%) = \frac{\text{mol of isoamyl acetate}}{\text{mol of isoamyl alcohol converted}} \cdot 100 \quad (3)$$

Therefore, the selectivity towards the byproduct (a ketal) is:

$$S_{\text{ketal}}(\%) = 100 - S_{\text{isoamyl acetate}} \quad (4)$$

Results and discussion

The H-ZSM-5 catalyst

Curve A in Fig. 1, shows the X-Ray powder diffraction pattern of Perlite, revealing its amorphous nature, while from Fig. 2 and Table 1 we conclude that this behavior is typical from a non-porous solid having a BET surface area of 2 $\text{m}^2 \text{g}^{-1}$. In a practically sense, this material has no micropores or mesopores and its low porosity must be explained fundamentally due the presence of macropores, generated

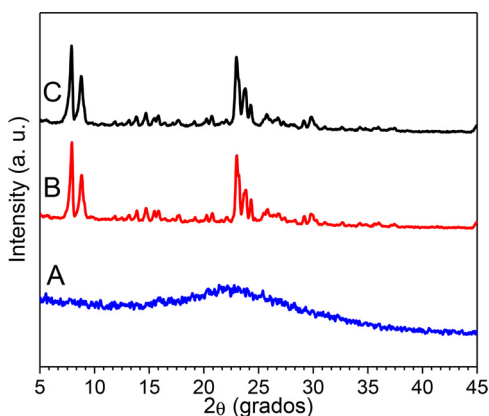


Fig. 1. XRD patterns. A) Perlite, B) the as-prepared ZSM-5, C) commercial ZSM-5.

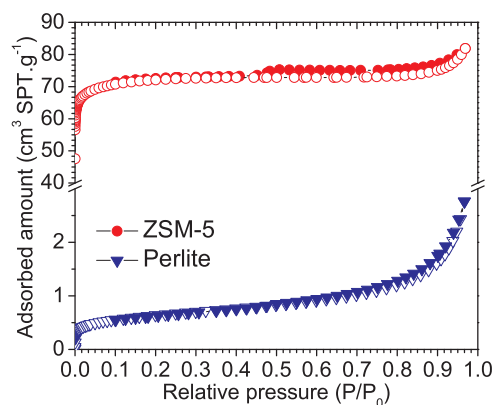


Fig. 2. Nitrogen adsorption isotherms.

Table 1

Surface area and porosity characteristics of expanded perlite and the as-prepared ZSM-5 zeolite.

sample	S_{BET} $\text{m}^2 \text{g}^{-1}$	Total pore volume ^a , V_{tot} ($\text{cm}^3 \text{g}^{-1}$)	Micropore volume, V_{mic} ($\text{cm}^3 \text{g}^{-1}$)		Mesopore volume, V_{Mes} ($\text{cm}^3 \text{g}^{-1}$)	Average pore ratio, r_p (nm)
			t -plot ^b	D.A. eq ^c		
Expanded Perlite	2	0.05	0.00	0.00	0.05	12.50 ^d
Na-ZSM-5	290	0.13	0.11	0.12	0.01 ^b - 0.02 ^c	0.55 ^c

^a At $p/p_0 = 0.99$ (Gurvitch rule).

^b t -plot method (Halsey model).

^c Dubinin-Ashtakov equation. ^d determined by BJH method.

during the thermal expansion process that was submitted. This process generates a sponge-like structure as evidenced in Fig. 3A.

On the other hand, the H-ZSM-5 displayed a nitrogen adsorption isotherm of type I, typical from a microporous material (Fig. 2) [19,20]. The hydrothermal treatment of Perlite generates a zeolite with a specific surface of 290 $\text{m}^2 \text{g}^{-1}$. Textural properties shown in Table 1 are in good agreement with those reported elsewhere [21–24].

The X-Ray diffraction pattern (Fig. 1, curve B) revealed no crystal phase other than ZSM-5, also having a good crystallinity as compared with a commercial ZSM-5 zeolite (Fig. 1, curve C). The SEM microphotographs exhibited well defined coffin-shape particles of nearly 6–7 μm large.

From the MAS NMR spectra of solid state (Fig. 4B) and according to Eq. (5), the Si/Al molar ratio was estimated as 38.5, where $I_{\text{Si}(n\text{Al})}$ is the peak area of the $\text{Si}(n\text{Al})$ signal in the spectra and n is the number of AlO_4 groups linked directly with the SiO_4 groups [25].

$$(Si/Al)_{\text{NMR}} = \frac{\sum_{n=0}^4 I_{\text{Si}(n\text{Al})}}{\sum_{n=0}^4 0,25 \cdot n \cdot I_{\text{Si}(n\text{Al})}} \quad (5)$$

Moreover, from the ^{27}Al MAS NMR, we consider that all Al is incorporated in the MFI framework as we evidenced a broad signal at 60–50 ppm in Fig. 4A, due to the tetrahedral coordination of Si. Also the absence of a peak at 0 ppm, unambiguously proves that there's no Al extraframework (i.e. octahedral coordinated) [25,26].

The number of Brønsted and Lewis acid sites were estimated using the integrated molar extinction coefficients (1.67 and 2.22 $\text{cm} \text{mol}^{-1}$) determined by Emeis [18], based on the intensities of the infrared absorption bands found at 1545 cm^{-1} and 1450 cm^{-1} , which correspond to the H-bonding pyridinium ion mode 19b and the coordinatively adsorbed pyridine [27–29], respectively. FTIR spectra of the as-prepared H-ZSM-5 sample after desorption of pyridine at three different temperatures are shown in Fig. 5. As was analyzed in our previous

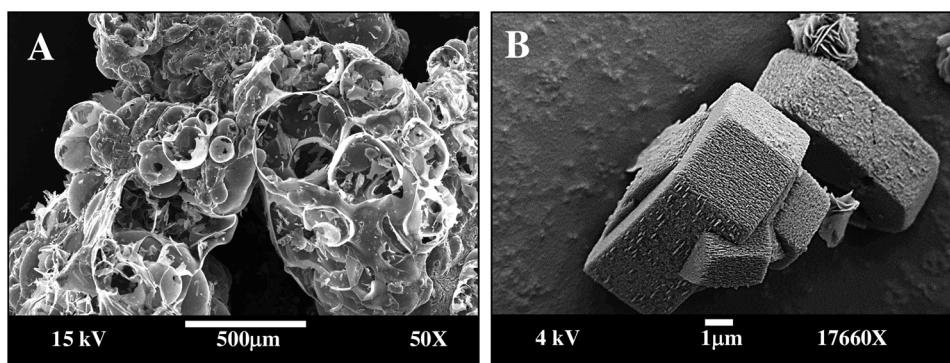


Fig. 3. SEM microphotographs. A) Expanded Perlite, B) the as-prepared ZSM-5.

paper [16], the concentration of Brønsted sites is 0.30 mmol of pyridine per gram. It is clearly shown that the area of the band at about 1545 cm^{-1} , related to Brønsted acid sites, is larger than that of the band at 1450 cm^{-1} . Therefore, the amount of Lewis acid sites is lower than the Brønsted one. The former is practically negligible compared to the latter. These findings are in agreement with the presence of only a tetrahedral Al signal in the ^{27}Al MAS NMR spectrum and also with the Si/Al molar ratio determined by ^{29}Si MAS NMR.

The Brønsted acidity showed a small variation after heating and a high amount of these acid centers still maintained pyridine bounded, revealing a strong surface acidity (Table 2). The moderate band observed at 1446 cm^{-1} , in the spectra at 323 K, should not be confused with the one assigned to Lewis acid sites, since the first practically disappears when temperature increases to 423 K. This behavior explains the desorption of weakly bounded pyridine due to interactions with silanol groups [27], which also agree with the presence of the HO–Si(O–Si) $_3$ signal at -102 to -108 ppm in the ^{29}Si MAS NMR spectra. Therefore, after desorption of pyridine from these weak centers, a band at 1451 cm^{-1} is observed due to the interactions of very small amounts of the probe molecule with Lewis acid sites. According to these results, we will consider in the following sections that the catalytic activity was due to the presence of Brønsted acid centers, exclusively.

The acyl transfer reaction: transesterification vs. ketalization

The transesterification reaction between vinyl acetate and isoamyl alcohol is shown in Scheme 1. This reaction is an example of a nucleophilic acyl substitution in which vinyl acetate possesses an electrophilic carbonyl carbon which also reacts with the nucleophilic isoamyl alcohol to give isoamyl acetate and vinyl alcohol. Although, as every alkenyl alcohol, vinyl alcohol undergoes a tautomerization into acetaldehyde. All reactants and products were detected in the gas chromatogram and the GC–MS analysis. These analysis also evidenced

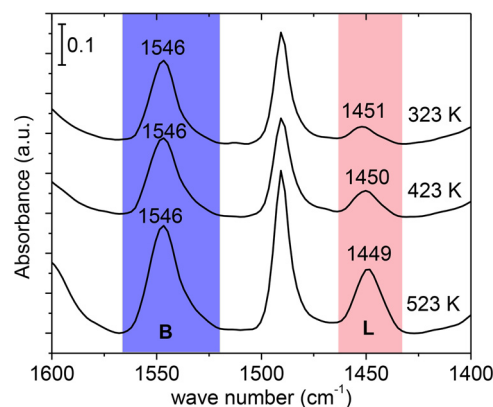


Fig. 5. FTIR spectra of pyridine adsorbed on the as-prepared H-ZSM-5 sample after pyridine desorption at different temperatures: 323, 423 and 523 K.

Table 2

Acidic properties expressed as the number of Brønsted and Lewis sites and percentage of Brønsted acid centers (ΔB_{Py}), referred to the initial amount at 323 K and saturated with pyridine at given temperature.

Temperature (K)	Brønsted (mmol g^{-1})	Lewis (mmol g^{-1})	ΔB_{Py} (%)
323	0.30	n.a. ^a	100
423	0.30	~ 0	100
523	0.26	~ 0	87
623	0.21	~ 0	71

^a n.a. = not applicable.

^b $\Delta B_{\text{Py}} = (\text{Number of Brønsted sites at certain temperature} / \text{Number of Brønsted sites at 323 K}) \times 100$.

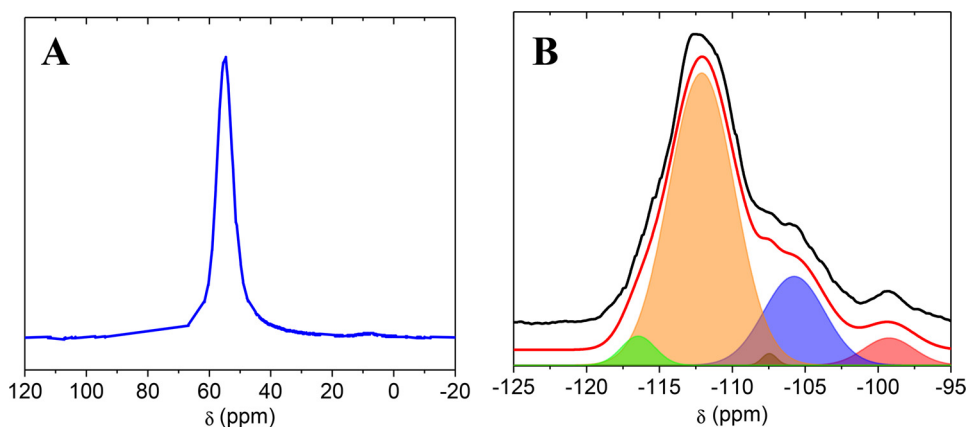
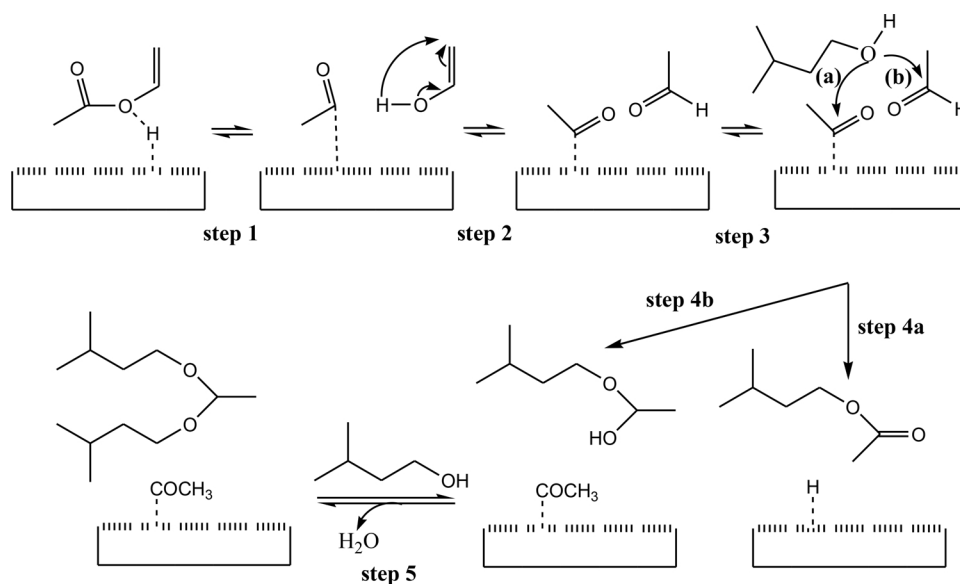
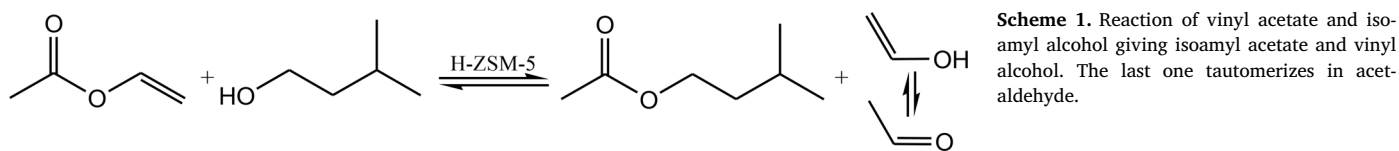


Fig. 4. NMR spectra of the as-prepared ZSM-5 zeolite. A) ^{27}Al -MAS NMR and B) ^{29}Si -MAS NMR: experimental spectra (black), calculated model (red) and Gaussian bands corresponding to the individual resonances (filled curves) obtained by deconvolution (For interpretation of the references to colour in this figure legend, the reader is referred to the web version of this article).



Scheme 2. Reaction path for the generation of products during the reaction of vinyl acetate and isoamyl alcohol catalyzed by H-ZSM-5.

the generation of a by-product having the IUPAC name of 1,1'-(ethyldenebis(oxy))bis(3-methylbutane), corresponding to the structure of acetaldehyde diisoamyl acetal (Scheme 2).

This secondary product is generated from the beginning of the reaction and at first, its signal in the chromatogram grows faster than the one corresponding to isoamyl acetate. This behavior must suggest that the nucleophilic attack of isoamyl alcohol to the electrophilic carbonyl carbon of acetaldehyde is faster than that of the vinyl acetate carbonyl carbon. Moreover, as we studied the reaction under catalyst-saturated conditions, an acyl-zeolite intermediate should be formed and thus, acting as the real acylating agent [14,30]. Therefore, we suggest that the acetal generation is faster than isoamyl acetate production as the nucleophilic alcohol can easily find an electrophilic center in the acetaldehyde carbonyl carbon. Instead of, the acetylated zeolite must generate isoamyl acetate when the nucleophilic agent cross the channel system and find the corresponding acyl ion interacting with the framework. Thus, a nucleophilic attack over the carbonyl carbon of the acetyl zeolite intermediate generates the desired product (isoamyl acetate).

Scheme 2 illustrates the proposed paths for the reaction under study. Since several authors [12–15,30,31] have reported the generation of an acyl-zeolite complex during acylation reactions using different acyl donors, we suggest at first, the formation of an acetylated surface from vinyl acetate adsorbed over a Brønsted acid center (step 1). This step also generates vinyl alcohol that quickly tautomerizes in a free acetaldehyde in step 2. Then, the approximation of isoamyl alcohol in step 3 has two possible electrophilic centers to attack: (a) the electrophilic center of carbonyl carbon in the acetyl-zeolite complex and (b) the electrophilic carbonyl carbon of free acetaldehyde. The reaction that follows path (a) generates isoamyl acetate in step 4a, while the attack according to route (b) produces a hemiacetal (step 4b) that further reacts with another mole of the nucleophilic agent to form the acetaldehyde diisoamyl acetal in step 5.

As mentioned before, the generation of the acetal seems to be the prime reaction at the beginning. This result is congruent with the

generation of a free acetaldehyde that easily reacts with isoamyl alcohol in a carbonyl nucleophilic addition. On the other hand, the generation of isoamyl acetate must occur exclusively inside the pores since the nucleophile (isoamyl alcohol) must find the acetylated zeolite complex, which then evolves to the desired product following an acyl nucleophilic substitution mechanism.

Moreover, we discard the generation of ionic species in the proposed reaction scheme, based in our previous results about the influence of solvents having different dielectric constant [32] over the mentioned reaction. We found that the conversion of the reaction is higher when using solvents with low polarity.

Influence of the concentration

Fig. 6A and B displayed graphs of conversion of alcohol and ester as function of time for different alcohol/ester molar ratios while Fig. 6C-D shows their respective conversion curves. These results indicate that an excess in the concentration of ester increments the conversion of vinyl acetate into isoamyl acetate, which can be explained considering that under a well-sealed system, a transesterification reaction remains at equilibrium state [2,3,33], governed by Le Châtelier Principle's. On the other hand, when increasing the alcohol/ester molar ratio from 1:1 to 2:1 and 3:1, at a constant concentration of vinyl acetate, the maximum conversion reached for vinyl acetate was 74, 85 and 98%, respectively.

The global chemical reaction including both, transesterification and ketalization can be expressed as detailed in Scheme 3.

The reaction under study does not have a simple kinetics. Thus, to establish the order of the reaction, we applied a graphical method [34,35] for the determination of the exponents of the general form of the rate Eq. (6):

$$v = k [\text{alcohol}]^{\alpha} [\text{ester}]^{\beta} \quad (6)$$

In excess of vinyl acetate, the α exponent was found to be 2, since a plot of $1/[\text{alcohol}]$ vs. time gives a straight line. Thus, the reaction is second order with respect of the isoamyl alcohol concentration.

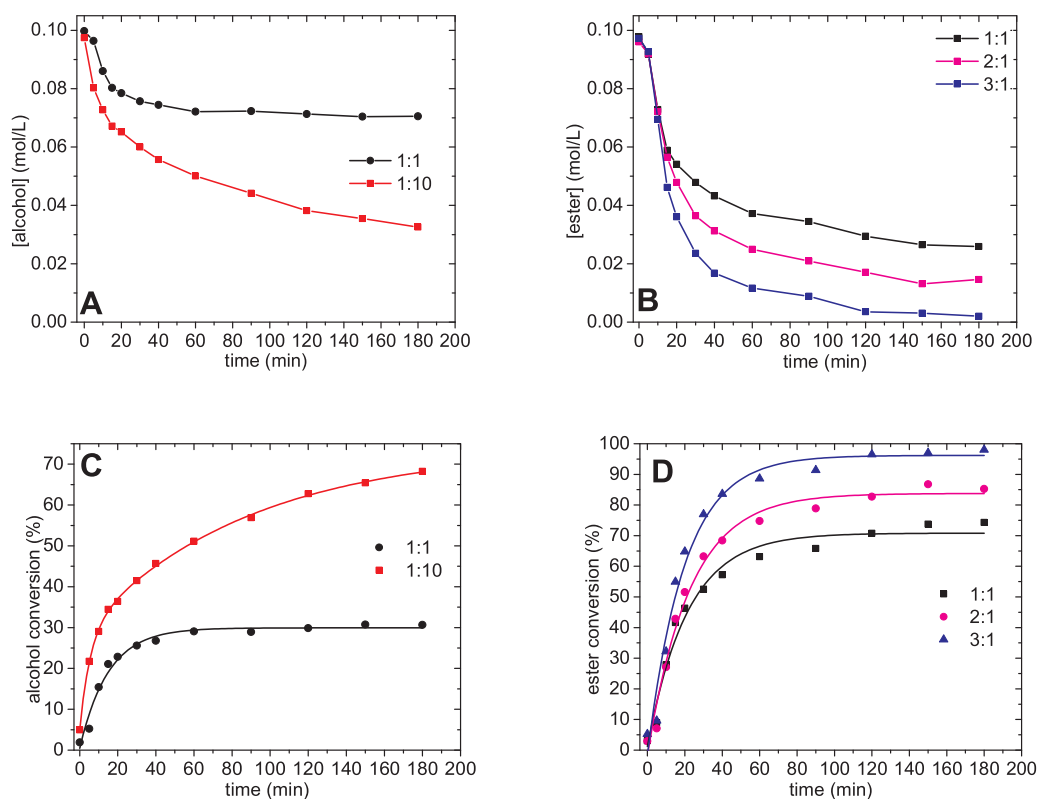


Fig. 6. Reaction profiles for the reaction of vinyl acetate and isoamyl alcohol. Effect of the concentration of ester (A, C) and alcohol (B, D).

Consequently, following the same methodology, the β exponent was found to be 2, meaning that the reaction is second order with respect of the vinyl acetate concentration when excess of isoamyl alcohol was used. In that sense, the global order for the studied reaction when using an excess of one reactant is 2 with respect of the limiting reagent. The rate law can be expressed as showed in Eq. (7), where ν is the rate of reaction ($\text{mol L}^{-1} \text{min}^{-1}$), k is the rate constant ($\text{L mol}^{-1} \text{min}^{-1}$) and the concentrations of reactants in mol L^{-1} are presented in square brackets.

$$\nu = k [\text{alcohol}]^\alpha [\text{ester}]^\beta \begin{cases} \beta = 2 & \text{If } [\text{alcohol}] \gg [\text{ester}] \\ \alpha = 2 & \text{If } [\text{ester}] \gg [\text{alcohol}] \end{cases} \quad (7)$$

The selectivity of the reaction presented in Fig. 7 shows not significant difference when considering the influence of the ester/alcohol molar ratio. A little excess at favor of isoamyl acetate was observed when working under equimolar conditions of alcohol and the acyl donor. Thus, concentration of reactants seems to not have influence in the selectivity of the reaction.

Moreover, turnover frequency (TOF), defined as the number of times that a catalyzed reaction occur per catalytic site in unit time, were calculated by following Eq. (8) and are listed in Table 4.

$$\text{TOF} = n_{\text{CH}_3\text{COOC}_5\text{H}_{11}} / (n_{\text{py}} \cdot m_{\text{cat}} \cdot t \cdot N_A) \quad (8)$$

In Eq. (8), n_{py} is the number of Brønsted acid sites in mol kg^{-1} determined by desorption of pyridine (py) followed by FTIR, m_{cat} is the mass of catalyst (kg), t is the reaction time (7200 s) in which the $n_{\text{CH}_3\text{COOC}_5\text{H}_{11}}$ molecules of isoamyl acetate were obtained and N_A is Avogadro's number ($6.022 \cdot 10^{23}$ acid centers mol^{-1}).

The TOFs are of great utility to compare activities of the same

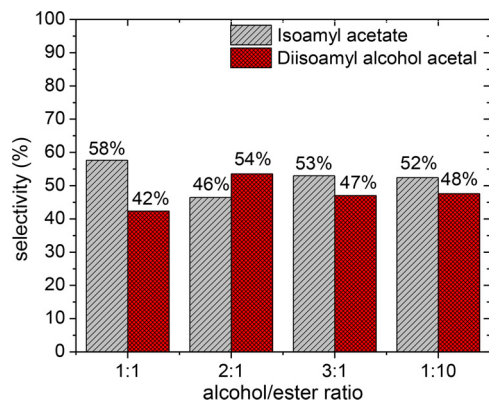
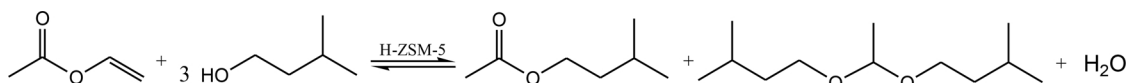


Fig. 7. Selectivity of the reaction.

catalyst under different conditions. The calculated values for TOFs are shown in Table 4, they are in good agreement with those reported for several reactions involving a ZSM-5 catalyst [36–40]. The catalyst has better activity when considering an excess of one reactant, which can be explained based in the reversibility of the reaction when maintaining a well closed system. In fact, an excess of one reactant will modify the equilibrium by displacing this state to the generation of products.

Moreover, in our intent to have a deep knowledge in the behavior of the catalyst, we studied some factors that influence the reaction, i.e. the regeneration and reuse of the catalyst. We find that it conserves approximately 70% of the activity in a fifth cycle of use, with respect to its original activity.



Scheme 3. Global reaction including transesterification and ketalization.

Table 3

Conditions for the study of the influence of concentration of vinyl acetate (Experiment A) and isoamyl alcohol (Experiment B) in the analyzed reaction.

	Effect of [Ester] (Experiment A)	Effect of [Alcohol] (Experiment B)
Mass of H-ZSM-5 catalyst (mg)	110	
Concentration of vinyl acetate (mol/L)	0.100	0.100
	1.000	
Concentration of isoamyl alcohol (mol/L)	0.100	0.100
		0.200
		0.300
Temperature (K)	363	
Alcohol/Ester molar ratio	1:1	1:1
	1:10	2:1
		3:1

Table 4

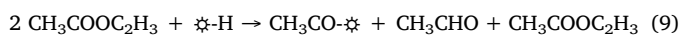
Turnover frequency values calculated at 7200 s for the influence of alcohol/ester molar ratio in the reaction of vinyl acetate and isoamyl alcohol.

Alcohol/ester molar ratio	TOF ($\times 10^{-4} \text{ s}^{-1}$)
1:1	8.3
2:1	11.6
3:1	14.7
1:10	17.2

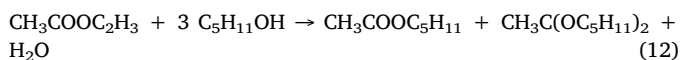
Kinetic model of the reaction

Considering that all of the Brønsted acid centers must be occupied by vinyl acetate molecules, the proposed mechanism of reaction follows an Eley-Rideal model. The adsorption of isoamyl alcohol over a catalytic site was not considered necessary as only the acyl donor must be adsorbed in order to generate the acyl zeolite complex. This specie will further suffer a nucleophilic attack from isoamyl alcohol as described earlier in this paper.

The kinetic model that fits the experimental results is the one that consider steps in Eqs. (9)–(11).



Where, $\text{CH}_3\text{COOC}_2\text{H}_3$: vinyl acetate; H : Brønsted acid centers of the catalyst; $\text{CH}_3\text{CO}-\text{H}$: acetylated zeolite complex; CH_3CHO : acetaldehyde; $\text{C}_5\text{H}_{11}\text{OH}$: isoamyl alcohol; $\text{CH}_3\text{COOC}_5\text{H}_{11}$: isoamyl acetate and $\text{CH}_3\text{C}(\text{OC}_5\text{H}_{11})_2$: acetaldehyde diisoamyl alcohol acetal. Thus, the addition of elemental reactions (9)–(11) gives the global reaction (12).



The first stage described by reaction (9) implicates the chemisorption of a vinyl acetate molecule to a Brønsted acid center on the catalyst. As we will discuss later in this section, this assumption will allow a reasonable description of experimental results as a second order reaction is needed when considering an excess of one reactant, thus demanding the value of 2 for the stoichiometric coefficient of vinyl acetate in step (9). The latter assumption suggests that not only one molecule of vinyl acetate will arrive to the acid center but also a second molecule will accompanied the first one, positioning the first molecule for the right interaction with the acid center. Once a molecule of vinyl acetate interacts with an active site in the catalyst, the other one will be closed to the first electronically attracted. At the same time, the isoamyl acetate molecule that interacts with a Brønsted acid center, quickly dissociates to produce the acetylated zeolite complex and acetaldehyde

(from tautomerization of vinyl alcohol). At that point, it is important to notice that a simple model can be assumed by considering that a molecule of vinyl acetate must be accompanied by another one, but also the same result must be anticipated in view of the accompaniment of more than one molecule. In fact, molecules associated will further be liberated and so, they will not participate directly in the reaction but only supporting the adequate orientation for the interaction between vinyl acetate and the Brønsted acid center.

On the other side, we assume that all chemical reactions are irreversible, thus the kinetic expressions of reaction rates (9) to (11) are respectively:

$$\rho_1 = k_1 [\text{CH}_3\text{COOC}_2\text{H}_3]^2 [\text{H}-\text{H}] \quad (13)$$

$$\rho_2 = k_2 [\text{CH}_3\text{CO}-\text{H}] [\text{C}_5\text{H}_{11}\text{OH}] \quad (14)$$

$$\rho_3 = k_3 [\text{CH}_3\text{CHO}] [\text{C}_5\text{H}_{11}\text{OH}]^2 \quad (15)$$

Moreover, considering that there's no accumulation of $\text{CH}_3\text{CO}-\text{H}$ and CH_3CHO , they must be consumed at same rate as they were produced, that means: $\rho_1 = \rho_2$ and $\rho_1 = \rho_3$. Thus,

$$k_1 [\text{CH}_3\text{COOC}_2\text{H}_3]^2 [\text{H}-\text{H}] = k_2 [\text{CH}_3\text{CO}-\text{H}] [\text{C}_5\text{H}_{11}\text{OH}] \quad (16)$$

$$k_1 [\text{CH}_3\text{COOC}_2\text{H}_3]^2 [\text{H}-\text{H}] = k_3 [\text{CH}_3\text{CHO}] [\text{C}_5\text{H}_{11}\text{OH}]^2 \quad (17)$$

Expressions (16) and (17) can then be rearranged as (18) and (19),

$$[\text{CH}_3\text{CO}-\text{H}] = k_1 [\text{CH}_3\text{COOC}_2\text{H}_3]^2 [\text{H}-\text{H}] / (k_2 [\text{C}_5\text{H}_{11}\text{OH}]) \quad (18)$$

$$[\text{CH}_3\text{CHO}] = k_1 [\text{CH}_3\text{COOC}_2\text{H}_3]^2 [\text{H}-\text{H}] / (k_3 [\text{C}_5\text{H}_{11}\text{OH}]^2) \quad (19)$$

Thus, the total balance for Brønsted acid sites can be represented by Eq. (20), where $[\text{H}-\text{H}]_{\text{total}}$ is a constant and equal to the total amount of acid sites.

$$[\text{H}-\text{H}]_{\text{total}} = [\text{H}-\text{H}] + [\text{CH}_3\text{CO}-\text{H}] + [\text{CH}_3\text{CHO}] \quad (20)$$

Then, the number of free Brønsted acid sites can be calculated by replacing expression (18) and (19) in (20), resulting in Eq. (21).

$$[\text{H}-\text{H}] = [\text{H}-\text{H}]_{\text{total}} / \left(1 + \frac{k_1 [\text{CH}_3\text{COOC}_2\text{H}_3]^2}{k_2 [\text{C}_5\text{H}_{11}\text{OH}]} + \frac{k_1 [\text{CH}_3\text{COOC}_2\text{H}_3]^2}{k_3 [\text{C}_5\text{H}_{11}\text{OH}]^2} \right) \quad (21)$$

The rate for the production of isoamyl acetate is given by ρ_2 and so, is also equals to the reaction rate (ν_R),

$$\rho_2 = \nu_R = k_2 [\text{CH}_3\text{CO}-\text{H}] [\text{C}_5\text{H}_{11}\text{OH}] = k_1 [\text{CH}_3\text{COOC}_2\text{H}_3]^2 [\text{H}-\text{H}]_{\text{total}} / \left(1 + \frac{k_1 [\text{CH}_3\text{COOC}_2\text{H}_3]^2}{k_2 [\text{C}_5\text{H}_{11}\text{OH}]} + \frac{k_1 [\text{CH}_3\text{COOC}_2\text{H}_3]^2}{k_3 [\text{C}_5\text{H}_{11}\text{OH}]^2} \right) \quad (22)$$

When the reaction is carried out in excess of isoamyl alcohol (i.e. $[\text{CH}_3\text{COOC}_2\text{H}_3] / [\text{C}_5\text{H}_{11}\text{OH}] = 1/10$, then $[\text{CH}_3\text{COOC}_2\text{H}_3]^2 / [\text{C}_5\text{H}_{11}\text{OH}]^2 = 1/100$), one can approximate Eqs. (22) to (23),

$$\nu_R \cong k_1 [\text{CH}_3\text{COOC}_2\text{H}_3]^2 [\text{H}-\text{H}]_{\text{total}} = k' [\text{CH}_3\text{COOC}_2\text{H}_3]^2 \quad (23)$$

Expression (23) describes the experimental behavior observed when studying the reaction in excess of isoamyl alcohol, which means, a second order kinetics with respects of vinyl acetate concentration.

As can be seen from Eq. (22), when $[\text{CH}_3\text{COOC}_2\text{H}_3] \gg [\text{C}_5\text{H}_{11}\text{OH}]$ and considering a similar procedure as described previously, one can arrive to expression (24) from (22).

$$\nu_R \cong k_3 [\text{H}-\text{H}]_{\text{total}} [\text{C}_5\text{H}_{11}\text{OH}]^2 = k'' [\text{C}_5\text{H}_{11}\text{OH}]^2 \quad (24)$$

Consequently, the kinetic expression (24) describes a second order reaction when the reaction is carried out in excess of vinyl acetate.

Conclusions

The reaction between vinyl acetate and isoamyl alcohol was studied over H-ZSM-5 zeolite catalyst, prepared by hydrothermal treatment of Expanded Perlite and as a greener route for the production of isoamyl

acetate. The as-prepared ZSM-5 zeolite offered a Si/Al molar ratio of 38.5, in which all the Al has been introduced into the framework and has exclusively Brønsted acids centers. The transesterification reaction that generates isoamyl acetate competes with the ketalization of acetaldehyde and isoamyl alcohol producing acetaldehyde diisoamyl acetal as a secondary product. The influence of reactants concentration developed a second order reaction with respect of the concentration of one reactant, when operated in excess of the other. A conversion of 98% was obtained by varying properly the concentration of reactants. A kinetic model was obtained for the reaction carried out under excess of one reactant. The kinetic model showed a second order kinetics which correlated well with the proposed Eley–Rideal reaction mechanism and also agree with the generation of an acyl zeolite intermediate complex proposed by several authors. The surface acylated intermediate further reacts under an acyl nucleophilic substitution to generates the desired product, while the nucleophilic addition to carbonyl carbon of acetaldehyde produces an acetal as a secondary product.

Acknowledgments

The authors gratefully acknowledge the financial support received as a grant from the Council of Researches of the Universidad Nacional de Salta (C.I.U.N.Sa.) (Projects N° 2301/0 and 2327/0).

References

- [1] E. Fischer, A. Speier, *Berichte der deutschen chemischen Gesellschaft* 28 (1895), pp. 3252–3258.
- [2] J. Otera, J. Nishikido, *Esterification: Methods, Reactions, and Applications*, Wiley, 2009.
- [3] J. Otera, *Chem. Rev.* 93 (1993) 1449–1470.
- [4] M. Paravidino, U. Hanefeld, *Green Chem.* 13 (2011) 2651–2657.
- [5] C.C. Akoh, L.N. Yee, *J. Mol. Catal. B Enzym.* 4 (1998) 149–153.
- [6] G.D. Yadav, A.R. Yadav, *Ind. Eng. Chem. Res.* 52 (2013) 10627–10636.
- [7] B.S. Balaji, B.M. Chanda, *Tetrahedron* 54 (1998) 13237–13252.
- [8] M. Sasidharan, R. Kumar, *J. Mol. Catal. A Chem.* 210 (2004) 93–98.
- [9] D. Srinivas, R. Srivastava, P. Ratnasamy, *Catal. Today* 96 (2004) 127–133.
- [10] H. Ogawa, T. Fujigaki, H. Saito, *Bulletin of Tokyo Gakugei University. Series IV, Mathematics and Natural Sciences* 56 (2004), pp. 53–56.
- [11] S.E. Collins, S.R. Matkovic, A.L. Bonivardi, L.E. Briand, *J. Phys. Chem. C* 115 (2011) 700–709.
- [12] A. Corma, M. JoséCliment, H. García, J. Primo, *Appl. Catal.* 49 (1989) 109–123.
- [13] O. Kresnawahjuesa, R.J. Gorte, D. White, *J. Mol. Catal. A Chem.* 208 (2004) 175–185.
- [14] M.L.M. Bonati, R.W. Joyner, M. Stockenhuber, *Microporous Mesoporous Mater.* 104 (2007) 217–224.
- [15] A. Gumidyala, T. Sooknoi, S. Crossley, *J. Catal.* 340 (2016) 76–84.
- [16] P.F. Corregidor, D.E. Acosta, H.A. Destéfani, *Sci. Adv. Mater.* 6 (2014) 1203–1214.
- [17] K.S. Triantafyllidis, L. Nalbandian, P.N. Trikalitis, A.K. Ladavos, T. Mavroumoustakos, C.P. Nicolaides, *Microporous Mesoporous Mater.* 75 (2004) 89–100.
- [18] C.A. Emeis, *J. Catal.* 141 (1993) 347–354.
- [19] K.S.W. Sing, *Pure and Applied Chemistry*, (1985) pp. 603.
- [20] S. Suganuma, K. Nakamura, A. Okuda, N. Katada, *Molecular Catalysis* 435 (2017) 110–117.
- [21] H. Belarbi, Z. Lounis, R. Hamacha, A. Bengueddach, P. Trens, *Colloids Surf. A: Physicochem. Eng. Aspects* 453 (2014) 86–93.
- [22] P. Wang, B. Shen, J. Gao, *Catal. Today* 125 (2007) 155–162.
- [23] P. Wang, B. Shen, D. Shen, T. Peng, J. Gao, *Catal. Commun.* 8 (2007) 1452–1456.
- [24] D.P. Serrano, J. Aguado, Á. Peral, *Controlling the Generation of Hierarchical Porosity in ZSM-5 by Changing the Silanization Degree of Protozeolitic Units*, in: A. Gédéon, P. Massiani, F. Babonneau (Eds.), *Studies in Surface Science and Catalysis*, Elsevier, 2008, pp. 123–128.
- [25] G. Engelhardt, D. Michel, *High-Resolution Solid-State Nmr of Silicates and Zeolites*, John Wiley & Sons, Australia, Limited, 1987.
- [26] L. Tortet, E. Ligner, W. Blanluet, P. Noguez, C. Marichal, O. Schäf, J.-L. Paillaud, *Microporous Mesoporous Mater.* 252 (2017) 188–196.
- [27] R. Buzzoni, S. Bordiga, G. Ricchiardi, C. Lamberti, A. Zecchina, G. Bellussi, *Langmuir* 12 (1996) 930–940.
- [28] M. Castellà-Ventura, Y. Akacem, E. Kassab, *J. Phys. Chem. C* 112 (2008) 19045–19054.
- [29] K. Sadowska, K. Góra-Marek, J. Datka, *Vib. Spectrosc.* 63 (2012) 418–425.
- [30] M.L.M. Bonati, R.W. Joyner, G.S. Paine, M. Stockenhuber, *Adsorption Studies of Acylation Reagents and Products on Zeolite Beta Catalysts*, in: E. van Steen, M. Claeys, L.H. Callanan (Eds.), *Studies in Surface Science and Catalysis*, Elsevier, 2004, pp. 2724–2730.
- [31] M.L.M. Bonati, R.W. Joyner, M. Stockenhuber, *Catal. Today* 81 (2003) 653–658.
- [32] P.F. Corregidor, *Faculty of Ciencias Exactas, Universidad Nacional de Salta, Salta, Argentina*, 2017, pp. 315.
- [33] E. Božek-Winkler, J. Gmehling, *Ind. Eng. Chem. Res.* 45 (2006) 6648–6654.
- [34] J.W. Moore, R.G. Pearson, *Kinetics and Mechanism*, Wiley, 1961.
- [35] G. Raj, Meerut-India, *Chemical Kinetics*, 8th ed., Krishna Prakashan media Ltd, 2010.
- [36] H. Konno, R. Ohnaka, J.-I. Nishimura, T. Tago, Y. Nakasaka, T. Masuda, *Catal. Sci. Technol.* 4 (2014) 4265–4273.
- [37] M. Lindén, F. Babonneau, H. Amenitsch, N. Baccile, A. Riley, S. Tolbert, *On the mechanism of formation of SBA-1 and SBA-3 as studied by in situ synchrotron XRD*, in: P.M. Antoine Gédéon, B. Florence (Eds.), *Studies in Surface Science and Catalysis*, Elsevier, 2008, pp. 103–108.
- [38] K. Suzuki, Y. Aoyagi, N. Katada, M. Choi, R. Ryoo, M. Niwa, *Catal. Today* 132 (2008) 38–45.
- [39] J. Wu, H. Zhu, Z. Wu, Z. Qin, L. Yan, B. Du, W. Fan, J. Wang, *Green Chem.* 17 (2015) 2353–2357.
- [40] H. Xin, X. Li, Y. Fang, X. Yi, W. Hu, Y. Chu, F. Zhang, A. Zheng, H. Zhang, X. Li, *J. Catal.* 312 (2014) 204–215.